UNCLASSIFIED

Defense Threat Reduction Agency
8725 John J. Kingman Road, MS
6201 Fort Belvoir, VA 22060-6201

DTRA-TR-20-58

TECHNICAL REPORT

Quantifying the Relationship Between Optical and Heavy-Ion-Induced Charge Generation

Distribution Statement A. Approved for public release; distribution is unlimited.
This report is UNCLASSIFIED.

Sept 2020

HDTRA1-16-1-0018

Prepared by: John Cressler

Georgia Tech
Atlanta, Georgia
30308

REPORT DOCUMENTATION PAGE

Form Approved OMB No. 0704-0188

1. REPORT DATE *(DD-MM-YYYY)*
16-09-2020

2. REPORT TYPE
Final report

3. DATES COVERED *(From - To)*
May 2016-Sept 2020

4. TITLE AND SUBTITLE
Quantifying the Relationship Between Optical and Heavy-Ion-Induced Charge Generation

5a. CONTRACT NUMBER

5b. GRANT NUMBER
HDTRA1-16-1-0018

5c. PROGRAM ELEMENT NUMBER

6. AUTHOR(S)
John. D. Cressler

5d. PROJECT NUMBER

5e. TASK NUMBER

5f. WORK UNIT NUMBER

7. PERFORMING ORGANIZATION NAME(S) AND ADDRESS(ES)
Georgia Tech
School of ECE
TSRB Room 521, 85 5th Street, NW, Georgia Tech, Atlanta, GA 30308

8. PERFORMING ORGANIZATION REPORT NUMBER
FR-GT 2106DPA

9. SPONSORING/MONITORING AGENCY NAME(S) AND ADDRESS(ES)
Defense Threat Reduction Agency
8725 John J. Kingman Road
Fort Belvoir, VA 22060-6201

10. SPONSOR/MONITOR'S ACRONYM(S)
DTRA

11. SPONSOR/MONITOR'S REPORT NUMBER(S)

12. DISTRIBUTION/AVAILABILITY STATEMENT
Distribution Statement A. Approved for public release; distribution is unlimited

13. SUPPLEMENTARY NOTES

14. ABSTRACT
The work produced as a result of this program has contributed to expanding the body of work related to establishing a quantitative correlation between pulsed laser data and heavy-ion data. The understanding of several fundamental concepts needed for this effort were significantly advanced. In addition, many experimental challenges required to tackle these problems were addressed (e.g., improved calibration of a laser system). The successful outcome of this program was largely due to the synergistic collaboration between the teams at Georgia Tech and NRL.

15. SUBJECT TERMS
radiation, SiGe, laser, heavy ion, single event transient, SET

16. SECURITY CLASSIFICATION OF: a. REPORT	b. ABSTRACT	c. THIS PAGE	17. LIMITATION OF ABSTRACT	18. NUMBER OF PAGES	19a. NAME OF RESPONSIBLE PERSON / 19b. TELEPHONE NUMBER *(Include area code)*
U	U	U	UU	27	John D. Cressler / 404-894-5161

DTRA Basic Research Final Report (May 2016 – Aug 2020)

Grant/Award #: HDTRA1-16-1-0018
PI Name: John D. Cressler
Organization/Institution: Georgia Institute of Technology
Project Title: Quantifying the Relationship Between Optical and Heavy-Ion-Induced Charge Generation

What are the major goals of the project?

Goals: To perform the basic research necessary to develop, and then to provide to DoD and the radiation-effects community, a framework for quantifying the relationship between the charge generation by laser-based nonlinear-optical (NLO) pulse injection and charge generation by heavy-ion irradiation in advanced semiconductor devices and circuits. Fig. 1 shows the fundamental difference in charge generation between a heavy-ion source, a single-photon source, and a nonlinear-optical pulse (such as two-photon absorption) which provides sub-bandgap photons that are highly penetrating until focused. We will leverage Georgia Tech's existing designs of state-of-the-art SiGe HBT and sub-100 nm strained Si CMOS hardware, at no cost to DTRA, to enable this comprehensive investigation. The device and circuit hardware will span multiple technology generations, and will be used to assess the impact of device structure, transistor topology (HBT vs. FET), doping profile (lateral and vertical), and scaling node, on the relationship between laser- and heavy-ion-induced charge generation, as it relates to the physics of SEE in devices, circuits, and ultimately DoD-relevant systems.

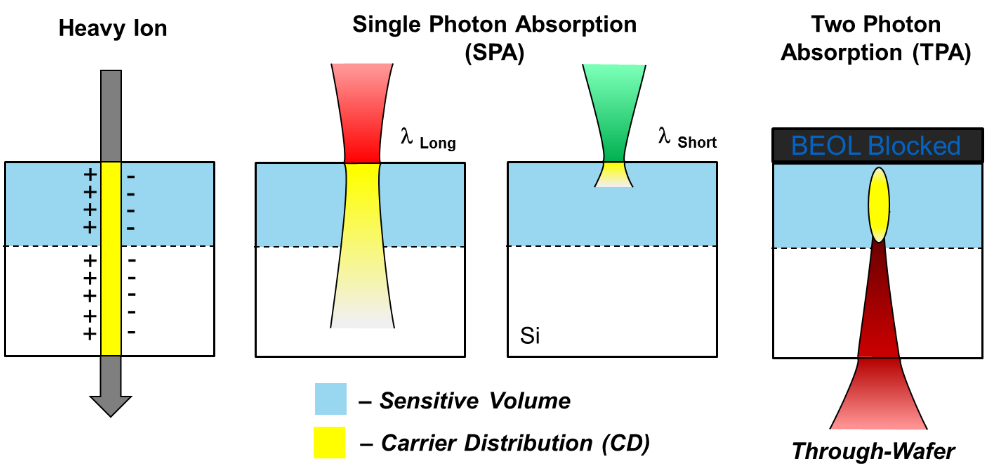

Fig. 1: Charge deposition profiles for heavy-ion and photon sources

Deliverables: This investigation will produce experimental results for single-event transients in advanced devices and circuits, using both laser and heavy ion sources, for: (1) large sensitive volume devices (e.g., diodes and SiGe HBTs), and (2) highly-scaled, small sensitive volume devices (e.g., 45 nm and 32 nm CMOS/SOI). We will incorporate the simulated output of the non-linear optical beam propagation method (NLOBPM) tool into calibrated technology computer aided design (TCAD) models for the device types measured. A quantitative comparison between simulated transients and measured transients will then be used to establish a mapping between laser energy and heavy-ion linear energy transfer (LET). This will lead to the development of a framework for other advanced semiconductor technologies (such as III-V's) to follow establishing nonlinear-optical (NLO) pulse injection as an additional tool for radiation hardness assurance.

What was accomplished under these goals?

For years, pulsed lasers have been shown to be an effective tool for probing the single-event response of microelectronic devices and circuits. Lasers have mainly been used for go/no-go tests such as determining whether a particular electronic component can latch up. Most studies on single-event transients have been qualitative in nature, examining general trends across circuit operating conditions. Due to the reduced cost and added accessibility of laser facilities compared with particle accelerators, establishing a quantitative relationship between ion and laser experiments would result in reduced cost and, potentially, in a reduced timeline for system development.

Throughout this program, we have developed several simulation, experimental, and data analysis techniques that directly increased our abilities to quantitatively correlate single-event transient (SET) waveforms resulting from optical- and heavy-ion-induced charge generation in several semiconductor platforms. A summary of significant results and annual milestones of this program is included below.

Results from Year 1

Year #1 Milestones:

- Conducted heavy ion beam experiments on SiGe HBT and CMOS/SOI transistors
- Conducted laser experiments on SiGe HBT and CMOS/SOI transistors
- Submitted Annual Report containing measurement data, analysis, and modeling results
- Published papers based on results (full list at end of this report)

Reference Sample Selection

The first step in this work was selecting appropriate samples to use when developing modeling, experimental, and data analysis techniques. After preliminary testing and simulation, two different samples were chosen. The first sample chosen was a first-generation silicon-germanium (SiGe) heterojunction bipolar transistor (HBT), referred to in parts of this report as a 'Golden' device. This device was chosen because of the large amount of studies published in the field of radiation effects (including total ionizing dose and single-event effects) at the device and circuit level, as well as device physics studies (including process modifications). Further, this device has been shown to have a sensitive volume that is similar in depth to most carrier density profiles induced with lasers by two-photon absorption (TPA). Thus, it serves as a challenging case to test modeling and experimental methods. A cross-section of the SiGe HBT 2-D model created using Synopsys Sentaurus, a TCAD tool, is shown in Fig. 2. The second device was a bulk silicon photodiode (Centronic OSD15-5T), which has undergone extensive laser, heavy-ion, and X-ray single-event effects (SEE) testing. This device has a large sensitive volume and can be leveraged to facilitate the development of new analytical and experimental techniques. Results for both devices will be shown throughout this report.

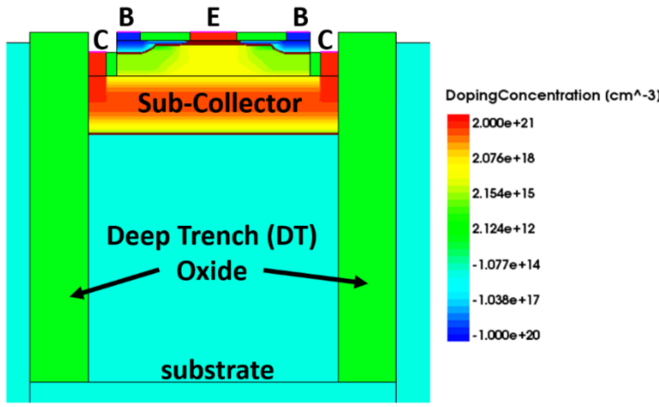

Fig. 2: 2-D TCAD model of the first-generation SiGe HBT with a CBEBC layout developed in Synopsys Sentaurus

Preliminary Heavy-Ion and Laser Experiments

During the first year of this program, four primary radiation experiments were conducted to investigate SETs in advanced SiGe HBT and CMOS electronics. These experiments were aimed at acquiring SETs in technologies of interest, and to aid in the creation of TCAD models that could be leveraged to compare differences between the radiation sources and experimental setups at different facilities. Heavy-ion experiments were conducted at the Lawrence Berkeley National Laboratory (LBNL) using the 10-MeV/amu cocktail in their 88-in cyclotron facility. In addition, pulsed laser testing was performed at the U.S. Naval Research Laboratory (NRL) using a wavelength of 1260 nm to induce carriers via TPA. The laser was focused from the backside of the die to prevent back-end-of-line (BEOL) metals from blocking the beam. Finally, an additional pulsed focused X-ray experiment was conducted at Argonne National Laboratory in Nov. 2016 (in collaboration with The Aerospace Corporation). This experiment adds a comparison of X-ray-induced charge generation to both heavy-ion and non-linear optical charge generation. Focused X-ray pulses generate charge using photons, but unlike typical focused laser experiments the higher photon energies are deeply penetrating and can traverse the BEOL metallization from the top side of the die. Based on the energy of the X-rays, one can describe an effective deposition range – much like that of a heavy-ion source.

Waveforms for the 'Golden' device acquired from several experiments, at the same bias, are shown in Fig. 3. These data show a clear difference in shape, particularly in the tail region of the SET. There is a clear relationship between the penetration of the source and the resulting magnitude of the tail and total charge deposition within the device. For experiments conducted at LBNL the range of a given ion is > 50 µm, whereas the range of a focused laser is in general much smaller for a tight spot size, although this may be changed by re-focusing the beam.

These preliminary experiments showed that matching the peak amplitude of the transients generated with ion and laser sources was relatively straightforward by simply adjusting the laser pulse energy, as shown in Fig. 4. However, these data also reveal a large disparity in the tail region of the device. This disparity was further investigated and resolved using additional experiments

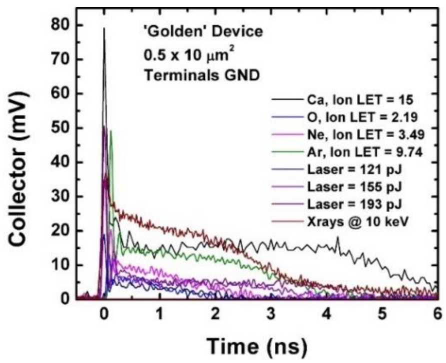

Fig. 3: Single-event transient waveforms for Heavy-ion, TPA Laser, and X-ray sources.

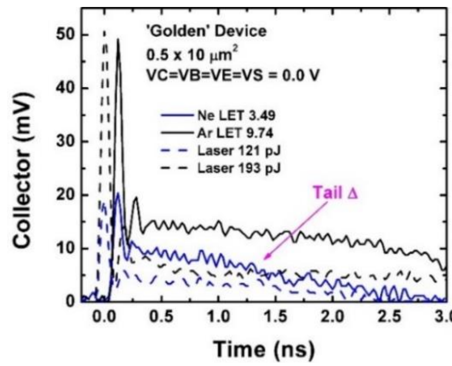

Fig. 4: Comparison of heavy-ion (Ne + Ar) SETs to TPA laser SETs in the 'Golden' device. Able to achieve peak transient matching in the experimental environment.

Preliminary TCAD Modeling Techniques

The first steps in developing modeling techniques for correlating ion and laser results was to create basic models in TCAD and get good matching for peak SETs in SiGe HBTs. These simulations used a superposition of modified heavy-ion models in Sentaurus TCAD to make a charge deposition profile that looks similar to that generated by TPA. The results of these first modeling efforts are shown in Fig. 5.

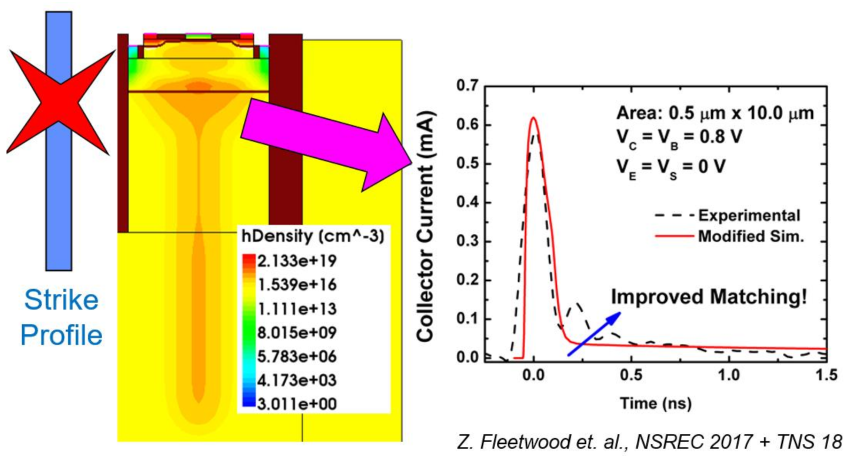

Fig. 5: Pseudo TPA charge model (left), injected into a 2D 'Golden' device model (middle), and the resulting waveform (right) compared to experimental TPA laser data.

Development of Analytical Charge Collection Models

Another concurrent area of work during this first year was the use and development of analytic charge collection models using NLOBPM. This work was conducted using the Centronic diodes with the goal of correlating heavy-ion and laser data. These analytic models show excellent agreement between ion and laser data, shown in Fig. 6, when using a laser-equivalent LET for single-photon absorption (SPA). One of the features of this approach is that very basic 1st-order rectangular-parallel-piped (RPP) approximations can accurately give researchers an indication of how much charge collection should be expected for a given laser energy without having to compute more advanced three-dimensional TCAD simulations, which can take on the order of hours or even days to complete. The analytic approach does have limitations and several assumptions have been made, including 100% charge collection efficiency. Some of these limitations have been addressed in the work done during subsequent years of this program

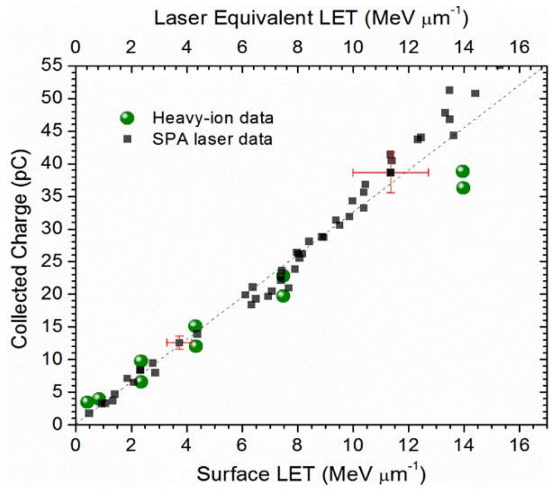

Fig. 6: Comparison of charge collection in a photodiode from both SPA laser and heavy-ion data. Laser data is mapped to heavy-ion energy using a 'Laser Equivalent LET' metric.

Results from Year 2

Year #2 Milestones:

- Conducted additional heavy ion beam experiments on SiGe HBT transistors
- Conducted additional laser experiments on SiGe HBT and CMOS/SOI transistors
- Developed TCAD modeling capabilities for improved comparisons with experimental data
- Submitted Annual Report containing measurement data, analysis, and modeling results
- Published papers based on results (full list at end of this report)

Improved TCAD Modeling

One of the main efforts during the second year of the program was to develop a calibrated 3-D TCAD model of our Golden device that could be used to simulate both heavy-ion- and laser-induced SETs. We found that a 3-D model was required to capture the long diffusion component of the SETs measured experimentally. The model was calibrated to DC and AC simulations from the foundry's process design kit. The structure of the device is shown in Fig. 7. In addition to this model, we also developed the capability for our group to create custom charge deposition profiles. These profiles could be imported either from

SRIM or NLOBPM to simulate the heavy-ion and laser charge deposition profiles more accurately. These improvements yielded adequate matching between the measured and simulated SETs.

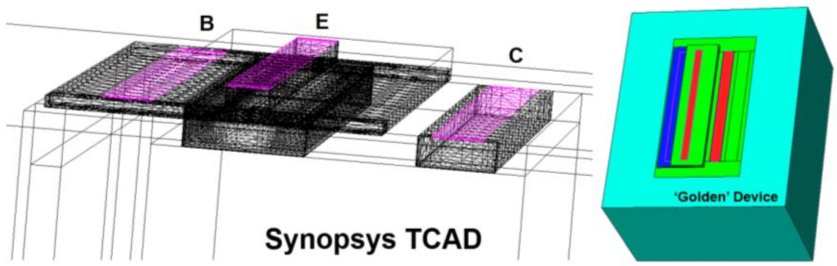

Fig. 7: 3D 'Golden' Device model in Synopsys's Sentaurus TCAD.

Additional Experiments to Correlate Ion and Laser Transients

Results from the previous year showed that it was easy to match transient amplitudes between ion and laser SETs, but the diffusion tail was much shorter for laser-induced transients compared to ion transients. Additional testing performed during the second year of this program using the same Golden device showed that either the peak magnitude of the transient waveform or the collected charge (i.e., the integrated transient current) could be easily matched by adjusting the laser pulse energy. However, when the same transient peak is obtained, the resulting collected charge for laser-induced transients was significantly lower than the heavy-ion transient. This is due to the previously observed mismatch in the "tail" of the transient, which is a slow component in the waveform resulting from carrier diffusion. As expected, when the collected charge is matched between laser- and ion-induced transients, which can be achieved by selecting the appropriate laser pulse energy, the resulting transient peak amplitude is larger for the laser-induced transients. These results are shown in Fig. 8. Thus, the focus of the second year of this project has been to obtain full waveform correlation between laser and heavy-ion data. This is essential before continuing to perform laser experiments on more complex circuits and systems.

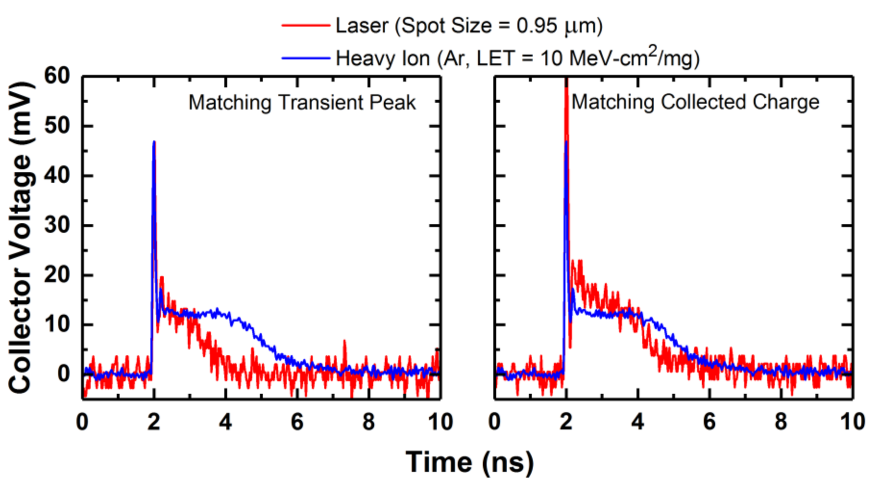

Fig. 8: Comparison of heavy-ion and laser transients in the 'Golden' device. With the existing experimental setup, either transient peak or collected charge can be matched by adjusting the laser energy, but not both simultaneously.

A trivial solution to enable correlation of SETs from these two sources would be to recreate heavy-ion charge deposition profiles using a laser. However, heavy ions used for SEE testing typically have a long range, necessary to support the constant-LET approximation, and the radial distribution of the resulting charge deposition is typically confined to several hundred nanometers. For a laser, the minimum achievable spot size is limited by several optical parameters (e.g., wavelength, focusing, and diffraction limit), and the Rayleigh range (analogous to the heavy-ion range), is proportional to the square of the spot size. Thus, an inherent tradeoff exists between matching the axial and radial charge deposition profile of a heavy ion. This difference can be observed in Fig. 9, where simulated charge deposition profiles for various optical geometries are compared to that of a heavy ion. Note that due to the rapid decrease in the charge density of the heavy-ion data, the logarithm of the data is plotted instead. The goal for correlating waveforms from different sources is to charge deposition profiles that result in the same measured transients.

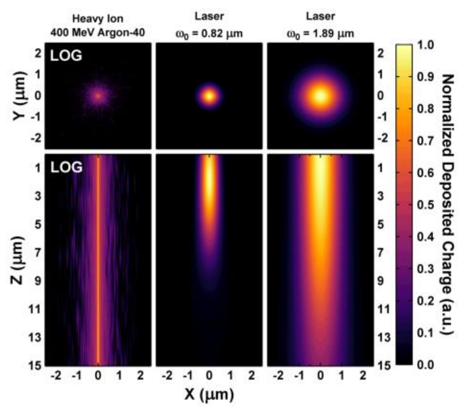

Fig. 9: Comparison of charge deposition profiles for (left) a 400 MeV Ar-40 ion, (center) focused laser with a 0.82 µm (HW1/e2) focused spot size, and (right) focused laser with a 1.89 µm (HW1/e2) focused spot size. Note that due to the rapid decrease in the radial charge density of the heavy-ion data, the logarithm of the data is plotted instead.

For these experiments, the laser focused spot size was varied between 0.82 µm and 1.89 µm by utilizing different microscope objective lenses. For each spot size, SETs were measured at different laser pulse energies. The resulting data set consists of transient waveforms as a function of laser spot size and energy. The heavy-ion data were measured at the 88-inch cyclotron BASE Facility at Lawrence Berkeley National Laboratory using the 10-MeV/amu heavy-ion cocktail. The transient peaks and collected charge were extracted for all laser and heavy-ion transients, and the SET waveforms were compared. We found that all heavy-ion transients were best matched using the laser when the focused spot size was set to 1.89 µm. The resulting matched waveforms are shown in Fig. 10.

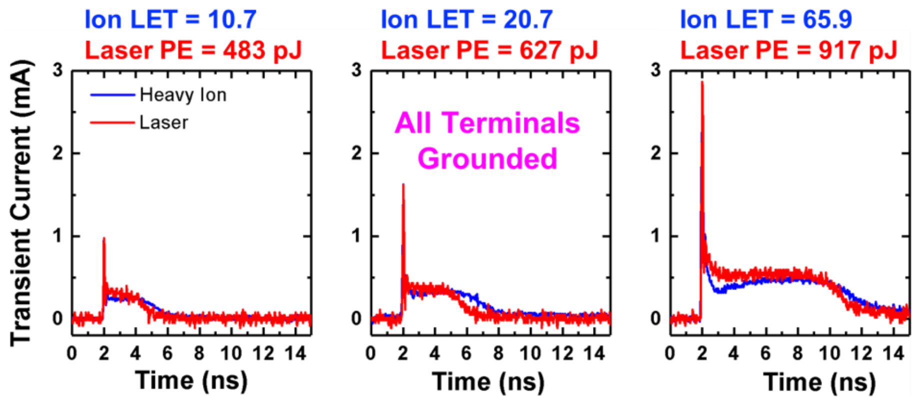

Fig. 10: Comparison of heavy-ion- and laser-induced single-event transients for multiple heavy-ion LETs and laser pulse energies. LET values are given in MeV-cm²/mg.

We also found that this waveform matching was possible because the relationship between transient peak amplitude and collected charge can be manipulated through a change in the laser spot size. The change in this relationship with varying spot sizes are shown in Fig. 11. The data show that for the spot size of 1.89 µm the dependence of the transient peaks on collected charge for laser transient matches that of ion transients. This is of great importance since it indicates that by fixing the spot size to some optimum point, the transients resulting from multiple ion LETs can be matched simply by changing the laser pulse energy, which is easily done at NRL's facility.

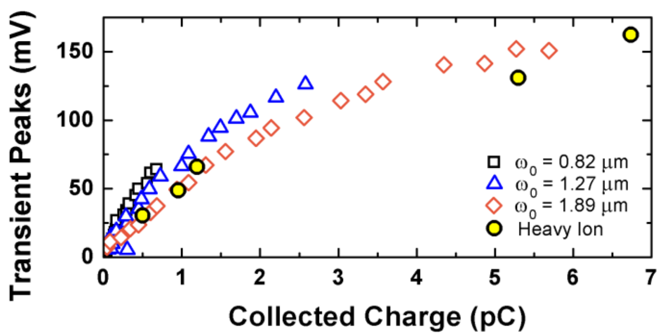

Fig. 11: Laser and ion-induced transient peaks as a function of collected charge. The data taken for a laser spot size of 1.89 µm shows the best match with heavy ion data.

Experimental Validation of the Laser-Equivalent LET

Another development of the work done during the second year was the experimental validation of the laser-equivalent LET (LE-LET). Since LET is the main metric used for heavy-ion testing, validating the concept of an LE-LET would be useful in these efforts. This approach uses a simplified rectangular parallelepiped (RPP) as a basis for calculating this LE-LET and has been applied to correlate collected charge in large photodiodes using both SPA and TPA. Fig. 12 shows the results of these studies where laser and ion data are compared and the excellent agreement between heavy-ion and laser-equivalent LET can be observed.

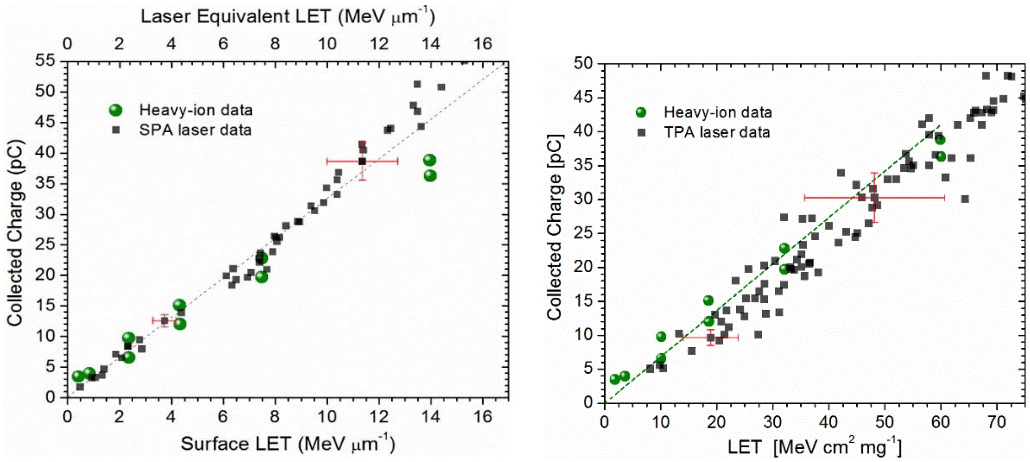

Fig. 12: Comparison of collected charge from heavy ion to (left) SPA and (right) TPA charge deposition on a large-area photo diode. Laser data is mapped to heavy-ion energy using a laser-equivalent LET and results in almost 1-to-1 correlation.

Although the results in Fig. 12 are for a large-area device, the same approach was applied to the Golden device, which is a high-performance SiGe HBT that is more relevant for DoD applications. The resulting comparison between the ion- and laser-induced collected charge is shown in Fig. 13. The data show excellent agreement through the LE-LET metric. In addition, with the application of the simultaneous match between collected charge and transient peak, the data shown in Fig. 13 will result in full waveform correlation.

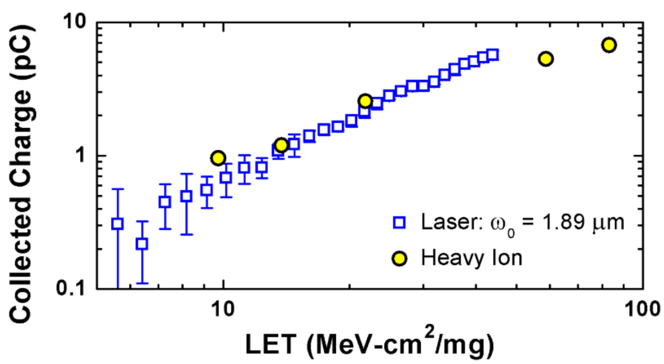

Fig. 13: Comparison of collected charge from heavy ion to TPA charge deposition on the high-performance Golden device.

Results from Year 3

Year #3 Milestones

- Conducted additional heavy ion beam experiments on SiGe HBT transistors
- Conducted additional laser experiments on SiGe HBT and CMOS/SOI transistors
- Developed TCAD modeling capabilities for improved comparisons with experimental data
- Developed new experimental approaches and techniques to facilitate ion/laser correlation
- Submitted Annual Report containing measurement data, analysis, and modeling results
- Published papers based on results (full list at end of this report)

A New Approach for Optimizing Optical Parameters to Facilitate Correlation of Laser- and Heavy-Ion-Induced SETs in SiGe HBTs

As previously mentioned, one of the challenges with correlating heavy ion and laser data is the difference in the resulting charge deposition profile from different sources. Work completed during the previous reporting year showed that by changing some of the parameters in the optical setup, in our case the focused spot size, we were able to achieve excellent correlation between ion- and laser-induced SET waveforms. This result was possible due to the manipulation of the relationship between transient peak amplitude and collected charge by changing the focused spot size.

During the third year, we extended the analysis of the previous experiments. More importantly, we developed a more general approach to achieve full waveform correlation, which we called "feature matching." In the context of this work, a "feature" is defined as a measurable or calculated property of an SET. For the SETs measured in SiGe HBTs, several features have been identified to fully describe the waveform: transient peak, transient full-width-at-half-maximum (FWHM), plateau height, transient duration, and collected charge. These features are illustrated in Fig. 14, where a representative heavy-ion-induced transient is used as an example. The goal of this method is to minimize the difference between features in a given ion-induced SET and laser-induced SETs by changing the optical parameters in the laser setup.

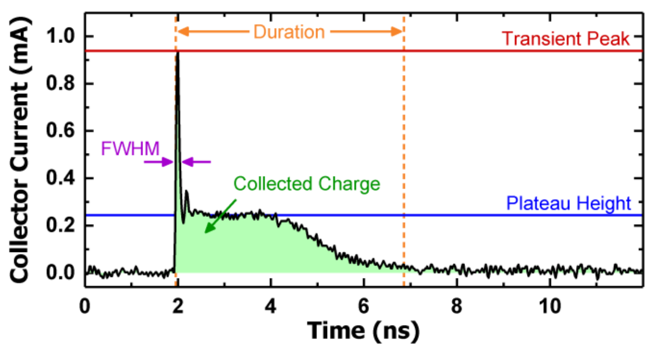

Fig. 14: Representative collector current transient taken from an emitter-centered strike of a 400 MeV Ar-40 ion (LET = 10.72 MeV-cm^2/mg). The main features of the heavy-ion-induced waveform are highlighted.

All the transients measured during the previous year were processed using a custom feature extraction algorithm that uses simple waveform analysis techniques. After analyzing the data, we determined that the transient peak amplitude, the plateau height, and the collected charge were the most relevant features to consider for our transients. The algorithm also calculated a difference error between features extracted from ion-induced and laser-induced SETs. A total error between SETs was calculated as an equal-weight sum of the magnitude of the individual error values. Using this approach, when the error between features is minimized, we can say that the waveforms matched. We can then use these optical parameters to reproduce the transient of a given ion. An example of the error values calculated is shown in Fig. 15. A similar analysis was performed for several worst-case ion-induced transients and a common optimum spot size of 1.89 µm resulted in the minimum error.

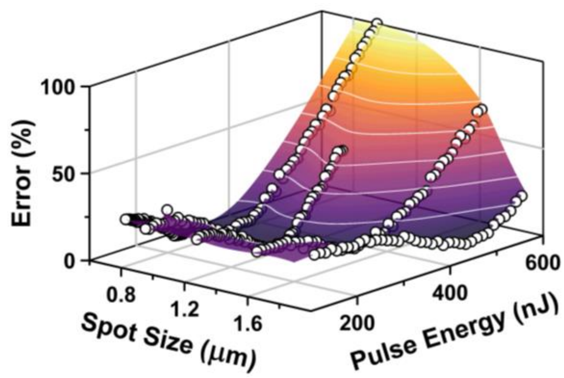

Fig. 15: The normalized error resulting from comparing features extracted from laser-induced transients to the worst-case, heavy-ion SET from a 400-MeV Ar-40 ion. A minimum error is achieved for a spot size of 1.89 μm and a pulse energy of 483 pJ.

The resulting matched waveforms for the Collector terminal have already been shown in Fig. 10. We also verified that the waveforms match in multiple device terminals and for the conditions when the device is biased (previous results are for when all terminals of the device are grounded). These matching waveforms are shown in Fig. 16. We found that this spot size results in a good correlation because the longer charge tracks generated by increasing the spot size can better reproduce the diffusion components present in SETs generated by heavy ions.

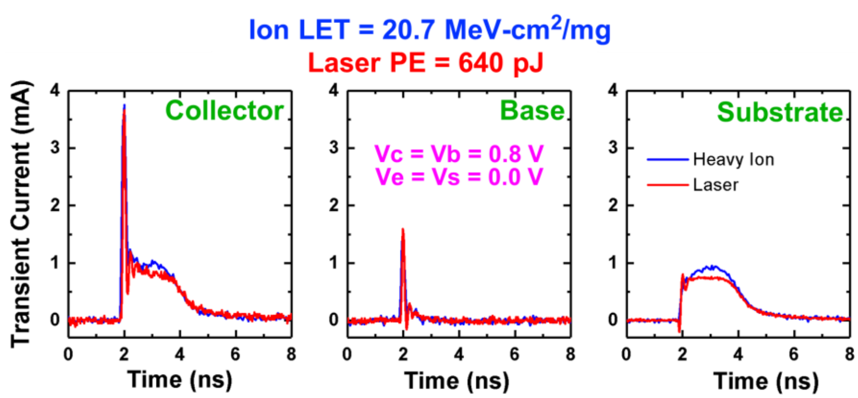

Fig. 16: Comparison of Heavy-Ion and Laser SETs for the collector, base, and substrate terminals of the SiGe HBT when the device is biased in forward-active mode.

After finding the optimized laser conditions that best reproduce ion-induced transients using a pulsed laser, the laser pulse energy is the only free experimental parameter. Therefore, pulse energy can be empirically correlated with heavy-ion LET. Fig. 17 shows LET values used in heavy-ion experiments, as a function of the laser pulse energy that best reproduces the ion-induced transient. The red dashed line in Fig. 17 is a linear fit to the experimental data. These results show an empirical relationship that allows us to determine the laser pulse energy needed to reproduce an ion with a given LET.

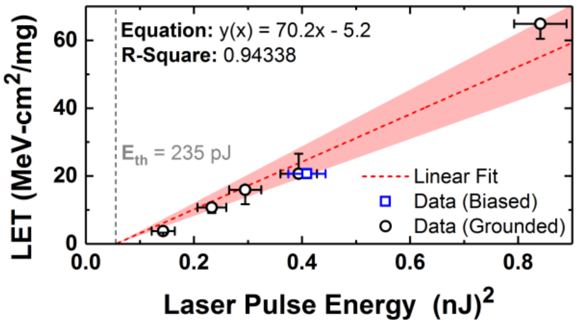

Fig. 17: LET used in experiment as a function of the pulse energy required to minimize the error between the respective ion and laser transients. The red dashed line shows a linear fit to the data.

Due to the generality of the presented framework, a similar approach can be performed for a variety of semiconductor devices and technology platforms. This ion/laser calibration process can lead to the creation of a "library" containing the optimal laser parameters for each technology platform, thereby allowing experimenters to obtain quantitative information on ion-induced transients from laser-based experiments at a fraction of the cost.

The results of this work were presented at the 2018 Nuclear and Space Radiation Effects Conference (NSREC) and the work was awarded the Outstanding Student and Outstanding Conference Paper Awards.

New Approach for Pulsed-Laser SEE Testing That Mimics Heavy-Ion Charge Deposition Profiles

In the previous study, we were able to correlate heavy-ion and laser SETs by increasing the spot size, which resulted in a longer track length. In a typical pulsed-laser setup, a microscope objective lens is used to generate a tightly focused beam. The spherical surface of the lens focuses the input light into a small spot, often described as a Gaussian beam. For a Gaussian beam, the track length is proportional to the square of the beam waist (i.e., what we call the focused spot size and the region of tightest focus). Thus, an inherent tradeoff exists between beam radius and track length. Most ions used for single-event effects testing produce a long charge track with a small radius. Thus, we proposed an alternative focusing geometry to better mimic charge deposition profiles generated by heavy ions.

Instead of a spherical surface, an axicon possesses a conical surface, which is the fined by its apex angle. This type of lens causes different portions of the input beam to be refracted toward each other, creating an interference pattern along the axis. The result is a cylinder-like beam with a small spot size. With this new focusing geometry, we can generate long charge tracks with a small radius. A diagram of the different charge deposition profiles generated from traditional focusing optics (using 100x and 20x microscope objectives), and from the axicon are shown in Fig. 18. Note that since the goal is to obtain long tracks with small radii, we can cite the aspect ratio of the beam as a figure of merit. The typical aspect ratio of a charge deposition profile resulting from heavy ions is close to 1000:1 (e.g., 100 µm long and 0.1 µm radius) For the 100x, 20x and axicon geometries the aspect ratios are 3:1, 9:1, and 1000:1, respectively. This schematic diagram shows that from the perspective of correlating ion and laser transients, using an axicon to focus the input light is an improved solution.

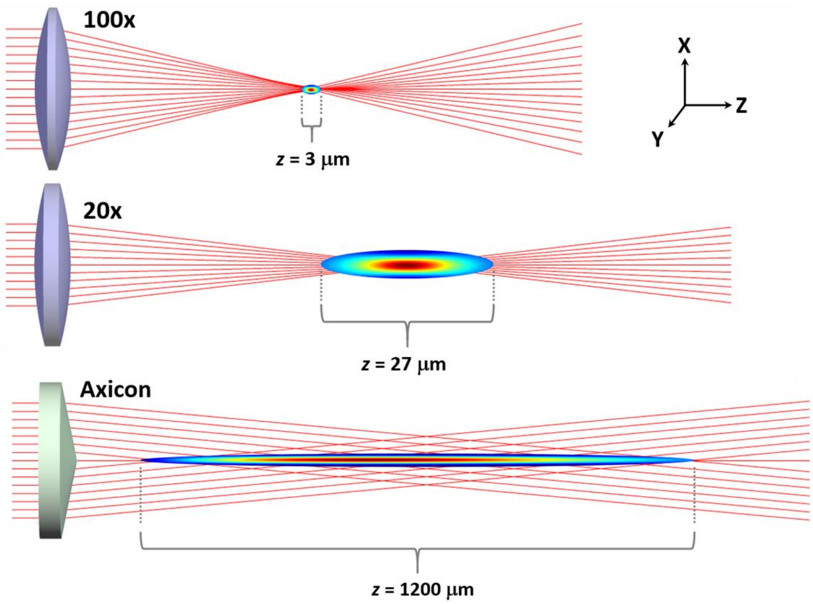

Fig. 18: Diagram of light being focused using a 100x objective, a 20x objective, and an axicon.

To verify that the beam generated by an axicon has the aspect ratio mentioned, SET testing of two samples were performed at NRL. First, we used a 45-nm SOI nFET to characterize the radial profile of the beam. Traditionally, this is accomplished using a knife-edge technique. However, since the beam is not directly sampled, the spatial resolution is usually insufficient for a micron-sized beam. Thus, we use a 45-nm SOI nFET to directly measure the beam. Since the sensitive area of this device is smaller than the beam, and since the response of this device depends linearly on the generated carrier density, scanning the beam in both X and Y directions allows us to spatially sample the intensity of the beam. The resulting beam profile is shown in Fig. 19

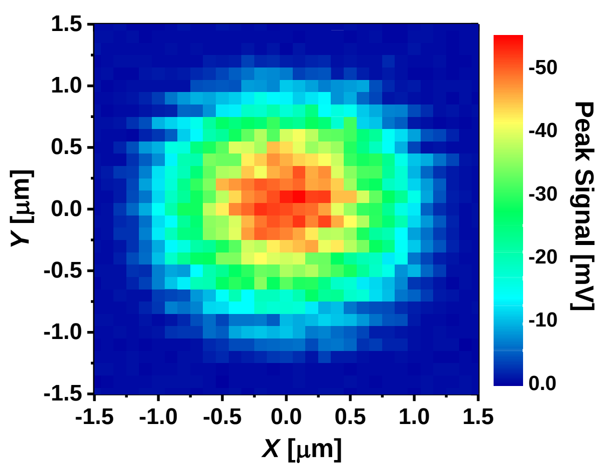

Fig. 19: Amplitude map of measured SETs in a 45-nm SOI nFET. Note that the beam has an approximate spot size of 1.9 μm.

After characterizing the beam in the radial direction using a small SOI nFET, we must characterize the beam in the axial direction. For this, we used a large Si diode because it possesses a deep charge collection depth (~66 μm) and a large surface area. This geometry ensures that the trends measured across focus depth are insensitive to the focused spot size. To characterize the beam in the axial direction (i.e., the track length), the beam was placed at the center of the Centronic Diode in the X and Y directions and was scanned in the Z direction. The results of this measurement are shown in Fig. 20. Note that the amplitude of the measured transient when using a 100x objective decays to 50% after moving the beam by 6 µm. In contrast, the transient amplitude decays by only 10% over an 800 µm range. This result combined with the measurements of the 45-nm nFETs show that we can use an axicon to generate charge tracks that are long in the axial direction and have a small radius.

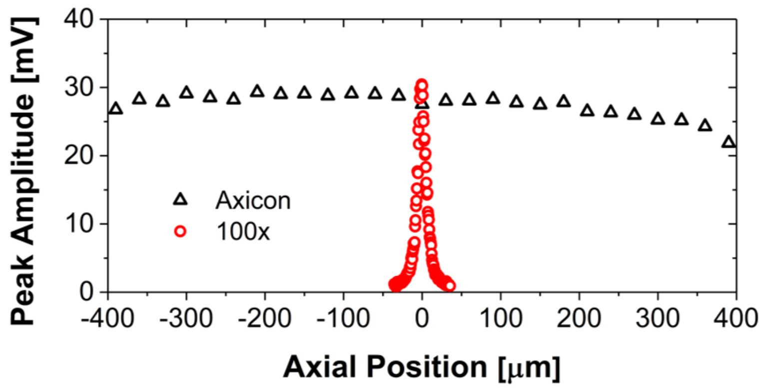

Fig. 20: Peak transient amplitude versus axial position of the bulk diode when the 100x objective and the axicon are used.

This geometry has larger potential to reproduce heavy-ion-induced transients using pulsed lasers. As an example, Fig. 21 compares the simulated rate of deposited charge for the 100x and the axicon beams with the LET profile of a Xe ion as a function of depth. These simulations show the similarities in the equivalent LET profile from the axicon and the Xe ion. Although more work needs to be done to verify the implications, the results suggest that correlating ion and laser transients should be more straightforward when using an axicon to generate carriers.

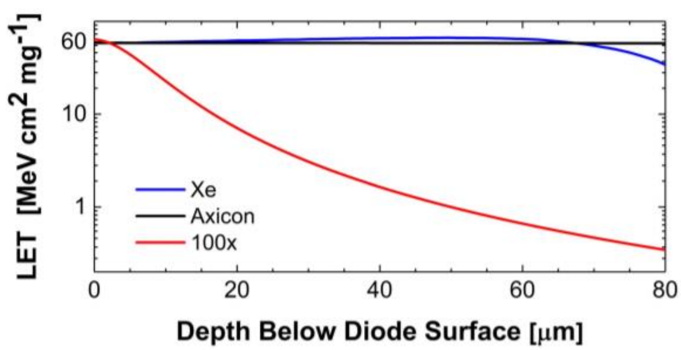

Fig. 21: Calculated LET curves produced by TPA in the bulk diode for the 100x objective and the axicon. These curves are compared to a SRIM-calculated LET curve for a Xe ion.

Results from Year 4

Year #4 Milestones

- Conducted additional laser experiments on SiGe HBT and CMOS/SOI transistors
- Improved TCAD modeling capabilities for improved comparisons with experimental data

- Continued validation of new experimental approaches and techniques to facilitate ion/laser correlation
- Developed data analysis techniques to facilitate ion/laser correlation
- Submitted Annual Report containing measurement data, analysis, and modeling results
- Published papers based on results (full list at end of this report)

Additional Verification of New Axicon Approach

During the previous reporting year, we developed a new experimental technique for pulsed-laser SEE testing that uses a conical lens known as an Axicon. Preliminary data showed that the spatial distributions of the carrier densities generated via this new testing approach more closely match those produced by heavy ions than the traditional laser testing approach. To further validate this technique and showcase its advantages, additional data were taken.

First, we examined the relationship between the transient peak amplitude and the collected charge, as we determined that this relationship is important when correlating data from different sources. Fig. 22 shows collected charge as a function of transient peak amplitude for transients induced by 1) heavy ions, 2) the traditional pulsed-laser testing technique (labeled 100x), and 3) the novel pulsed-laser testing technique using the Axicon. The data show that transients generated by the Axicon accurately reproduce the relationship between collected charge and amplitude that is obtained from heavy ion data. The ability to reproduce this relationship allows us to match ion and laser transients only by adjusting the laser pulse energy.

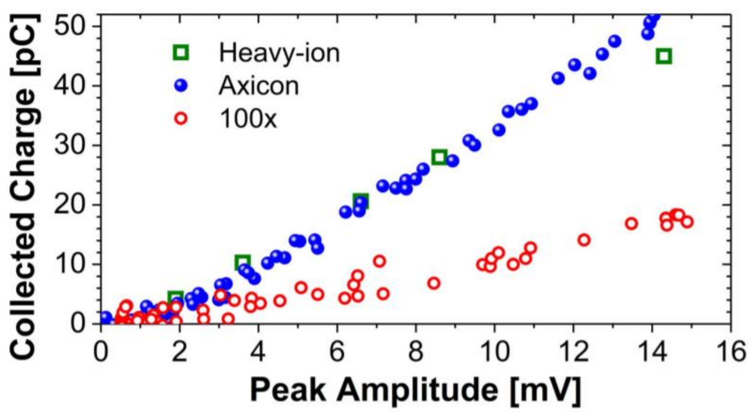

Fig. 22: Collected charge as a function of peak transient amplitude for data measured using heavy ions, the traditional pulsed-laser approach (labeled 100x), and the new pulsed-laser approach (labeled Axicon).

A comparison of the transients resulting from measurements using both heavy ions and the new Axicon pulsed-laser testing approach is shown in Fig. 23. The data show excellent agreement between the ion and laser data over the wide range of ion LETs measured. More importantly, because of the simple shape of the carrier densities generated by the Axicon, the process of calculating the LE-LET becomes more straightforward, which is one of the clear advantages of using this new testing technique. The calculated LE-LET is shown in the legend of each plot and is very similar to the ion LET. Although this technique needs to be validated in other platforms, it holds promise for a more straightforward approach to facilitate the correlation of ion and laser data.

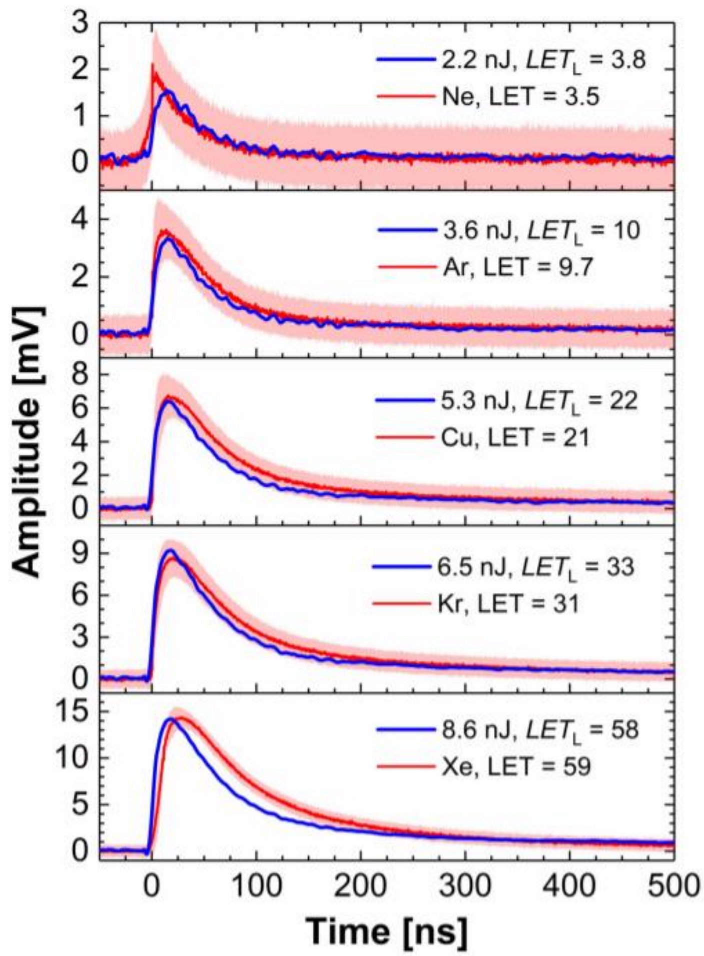

Fig. 23: Comparison of SETs generated by heavy ions and pulsed-laser testing. The data cover a wide range of ion LETs and laser pulse energy and show excellent agreement between the two sources.

Comparison of SETs in SiGe HBTs on Bulk and SOI Substrates

Given the past challenges with matching the transient tail between heavy-ion and laser data in SiGe HBTs, we compared the SET response of the same device fabricated on both bulk and silicon-on-insulator (SOI) substrates. Because the tail component is a result of charge diffusion from the substrate, fabricating these devices on SOI would remove this component. Removing this component would, in turn, simplify efforts to correlate laser and ion data. To verify this claim, identical samples were designed and fabricated using the Jazz SBC18H3A and SBC18H3B platforms. The SiGe HBTs in both processes are identical, and the main difference is the substrate (i.e., one is bulk, and the other is SOI). The samples were taken to LBNL and NRL, where we performed similar experiments as with other samples. A comparison of the difference between the bulk and SOI transients for two different ions is shown in Fig. 24

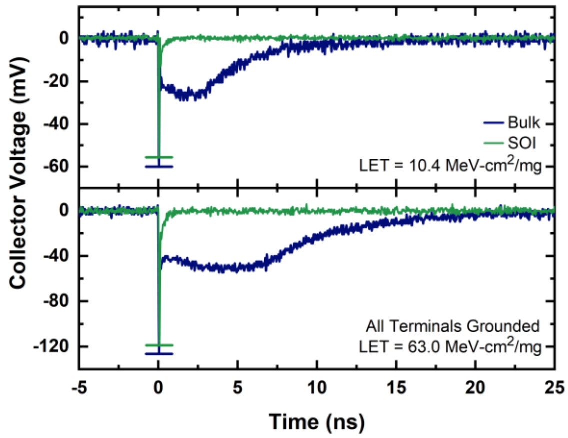

Fig. 24: Measured collector transients in SiGe HBTs on bulk and SOI for Ar (top) and Xe (bottom) ion beams when all terminals on the device were grounded. The horizontal lines indicate the transient peak amplitude for each waveform.

As expected, the transients for the bulk device exhibit the traditional long diffusion tail which is missing in the transients for the SOI device. It is worth noting that the worst-case transient peak amplitudes were similar between both devices for the ions used during this experiment. This phenomenon is thoroughly discussed in the IEEE TNS publication associated with this work.

We also compared the measured heavy-ion SETs to laser-induced transients to verify our theory that the SOI transients would be simpler to match due to the removal of the diffusion tail. The results of this comparison are shown in Fig. 25. The data show that, for the optical geometry used, there is a large discrepancy between the ion and laser transients for the bulk device, but the resulting transients from both sources are almost identical for the SOI device. Note that no attempt to optimize the laser spot size was made for this experiment. Thus, without any additional effort, the ion and laser waveforms for the SOI sample can be matched simply by tuning the laser pulse energy and matching the peak amplitudes.

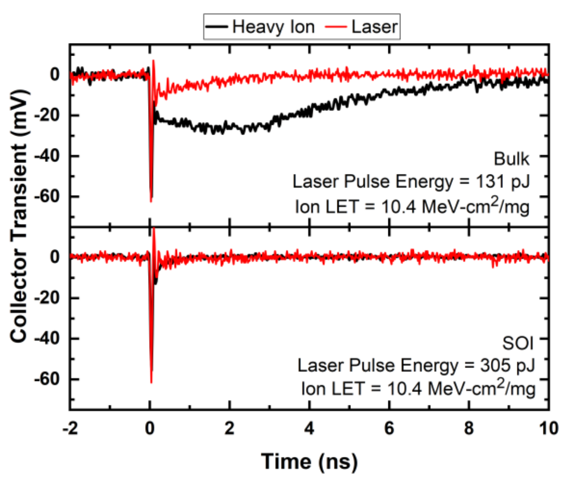

Fig. 25: Comparison between laser- and ion-induced transients in bulk (top) and SOI (bottom) SiGe HBTs when the samples are exposed to an Ar ion and all terminals of the device are grounded. Note that there are significant differences between the ion and laser transients for the bulk device, but the transients for the SOI device are almost identical.

SETs in SiGe HBTs Induced by Pulsed X-Ray Microbeam

In an interest of isolating any discrepancies between charge deposition via particles (i.e., heavy ions) and photons (i.e., lasers), an additional experiment using a pulsed X-ray microbeam was performed. This experiment was done at the Argonne National Laboratory in collaboration with The Aerospace Corporation. This facility generates a pulsed X-ray that has been focused down to a spot of several microns. Since X-rays are deeply penetrating, this technique would be analogous to using something like an Axicon during pulsed-laser testing. These experiments were performed using a 3rd-generation SiGe HBT fabricated in GlobalFoundries' 8HP platform.

The data from this experiment showed a large discrepancy in the transient shape between heavy ions and pulsed X-rays. An example of this discrepancy is shown in Fig. 26. After careful study, the differences between these waveforms were attributed to the relatively low carrier densities generated by the X-ray beam in comparison to a heavy ion. Such lower carrier densities will not be enough to shunt the emitter-base-collector stack, an event which gives rise to the fast and large transient peak observed in these devices. Further, since the lower carrier densities do not collapse the electric field in the collector-substrate junction as strongly as an ion, the deposited charge is collected more quickly, resulting in a faster diffusion tail, which is now assisted by the electric field in the junction.

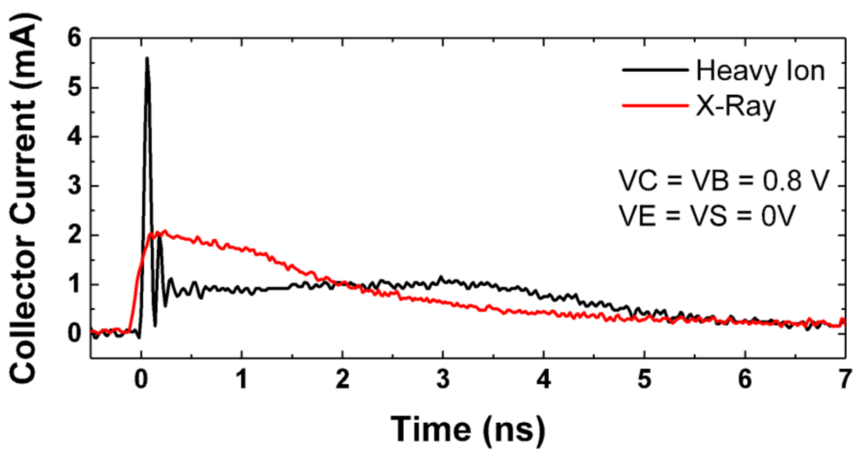

Fig. 26: Comparison of heavy-ion- and X-ray-induced SETs for the collector terminal when the device is biased at VC = VB = 0.8 V, VE = VS = 0 V.

However, despite these differences in waveform, we were able to correlate the collected charge between heavy-ion and X-ray transients by calculating an equivalent surface LET for the X-ray data. The results of this comparison are shown in Fig. 27 and the data show excellent agreement between both sources. This result allows us to still use pulsed X-ray data to evaluate circuits that might be sensitive to the amount of collected charge.

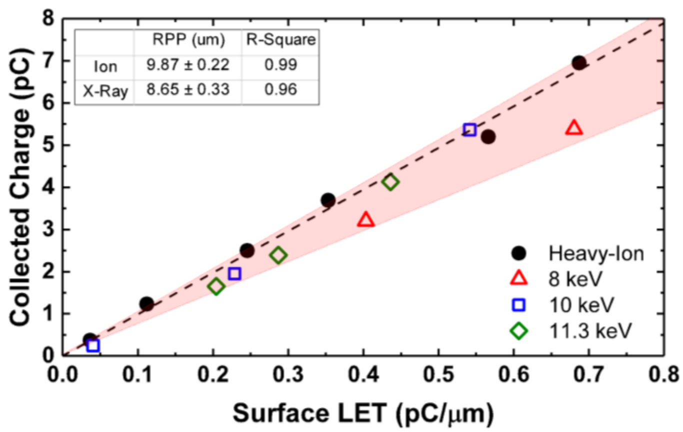

Fig. 27: Collected charge for both X-ray and heavy ion data as a function of surface LET.

An example of a circuit that is sensitive to collected charge is a shift register. In a digital circuit such as a shift register, a single-event upset (SEU) will occur when the collected charge exceeds a critical charge. This critical charge often depends on the circuit topology and the fabrication process, and dictates how sensitive a given design is to upsets caused by heavy ions. To evaluate the efficacy of using this tool for the purpose of identifying sensitive components in a system, the X-ray microbeam was scanned multiple times across four D flip-flops in a 16-bit shift registers. The number of upsets at each position of the X-ray beam was recorded and is mapped to the layout of the design in Fig. 28. In this plot, the bit upsets occur mostly on the D flip-flops, while no bit upsets are observed in the hardened clock buffers. This spatial map of bit upsets shows the most sensitive component of this shift register. For a designer, this information is valuable to determine the components of the circuit where radiation hardening techniques should be implemented.

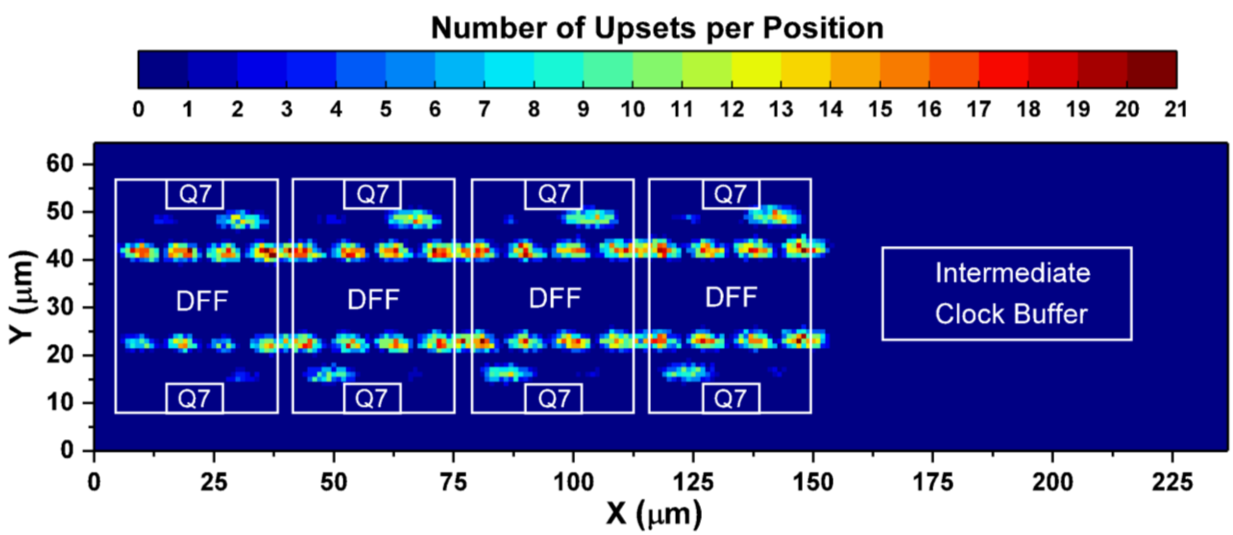

Fig. 28: SEU raster scan of a 16-bit MS shift-register. The scan was taken on four of the sixteen D flip-flops and one of the four clock buffers. No upsets were measured when the beam was scanned across the clock buffer because it was hardened using the gated-feedback cell technique.

Experimental Extraction of Charge Collection Efficiency Using Laser Data

Charge collection efficiency (CCE) is a key parameter in determining charge collection in a device. It is a measure of the fraction of the deposited charge that is collected at a junction. Typically, CCE is represented as a single number relating the total deposited charge to the total CC. In reality, CCE exhibits a 3-D spatial dependence since it is a function of the distance to the sensitive node. The concept of CCE is also important in the context of correlating ion and laser data, as it can inform the proper selection of charge deposition profiles using a laser that would result in similar collected charge from ions. However, it is difficult to determine the spatial dependence of the CCE for a given device without intimate knowledge of the device structure and doping parameters. Thus, we are developing a technique that uses pulsed-laser testing to extract the spatial dependence of CCE. The method relies on moving the focus of a Gaussian beam across a device and using the different measured values of collected charge in conjunction with calculated values for deposited charge to extract collection efficiency. The work on developing this method is still in progress, but preliminary results have yielded experimental CCE curves that provide information that is more useful than the traditional RPP approximation. One such curve obtained from the Centronic diode is shown in Fig. 29. Overall, this method could provide insight into the fundamental mechanisms of charge collection in devices, help facilitate threshold estimates in SEU and SEL studies, and improve modeling efforts through the introduction of non-discretized sensitive volumes.

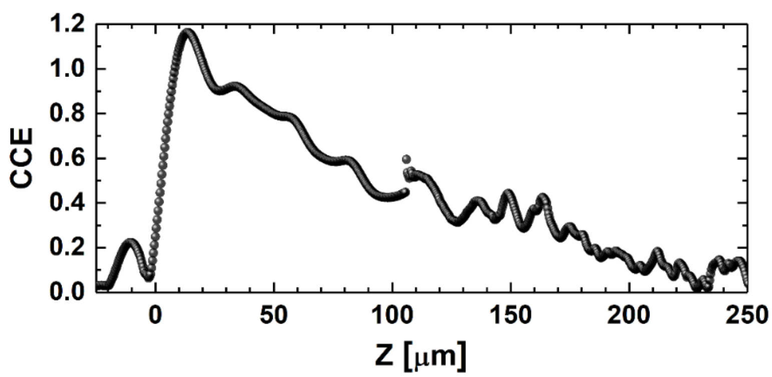

Fig. 29: Experimentally extracted charge collection efficiency (CCE) as a function of depth for a Centronic bulk diode.

Comparison of SETs in SiGe HBTs using Gaussian and Quasi-Bessel Beams

Since the pulsed-laser charge deposition technique that uses the Axicon is new, it should be validated using a variety of device types and platforms. Thus, to begin this effort, the SETs for a 3rd-generation SiGe HBT (GlobalFoundries' 8HP) resulting from heavy ions and pulsed lasers were compared. For the laser experiments, both the traditional technique (i.e., Gaussian beam) and the new technique (i.e., quasi-Bessel beam) were used. The preliminary results of these experiments are shown in Fig. 30, which shows a comparison of the SETs produced by all three experimental techniques. It is important to note that no attempt was made to optimize the spot size for either of the pulsed-laser experiments. These data show that better agreement with the ion data is obtained by the waveforms produced with a Gaussian laser beam than the new Bessel beam.

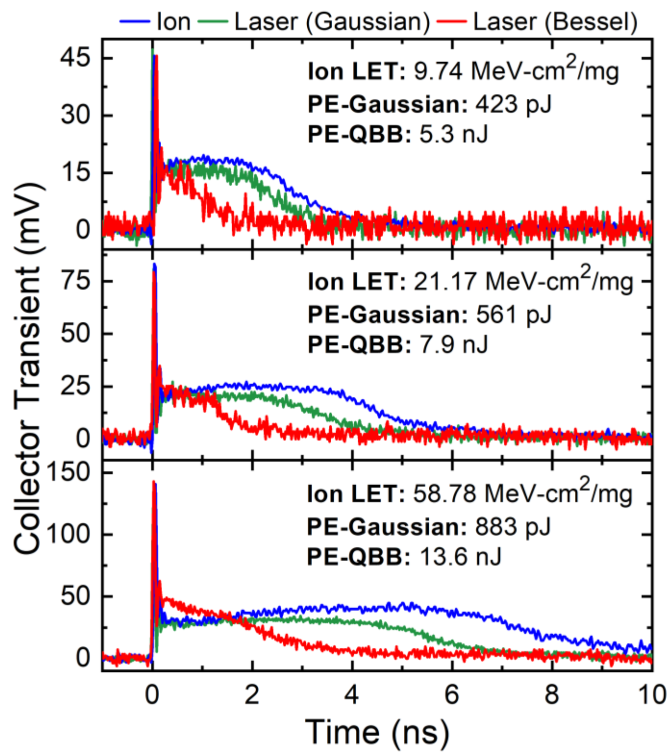

Fig. 30: Measured transients for a heavy ions, a Gaussian laser beam, and a quasi-Bessel laser beam for various ion LETs and laser pulse energies. The data for each panel were chosen based on matched transient amplitude.

This puzzling result was confirmed by examining the relationship between transient amplitude and collected charge, as has been shown for previous results in this report. This relationship is shown in Fig. 31 for all three experimental setups. The data again show that the relationship between peak amplitude and collected charge of the heavy-ion data is better reproduced by the Gaussian beam than the Bessel beam. Although these results are preliminary and additional work must be completed to confirm the source of this discrepancy, preliminary simulations suggest that these differences can be attributed to the funnel effect. This effect has been widely described in the literature and occurs when the spatial distribution of the electric field in a junction is distorted as a result of charge being deposited, leading to a "funneling" of the electrostatic potential. The differences in funneling between the Gaussian and Bessel beams have been simulated and are shown in Fig. 32. The deeper funnel generated by the Bessel beam compared to the Gaussian beam would result in charge being collected on a shorter time scale, which leads to higher amplitudes for a given collected charge.

Although we are still exploring alternative explanations and will collect more data to verify these claims, the data strongly suggest that despite the longer charge tracks generated by the Bessel beam, there may be an optimum spot size to reproduce ion results, as was the case with the Gaussian beams. This possibility will be further explored in a future experiment.

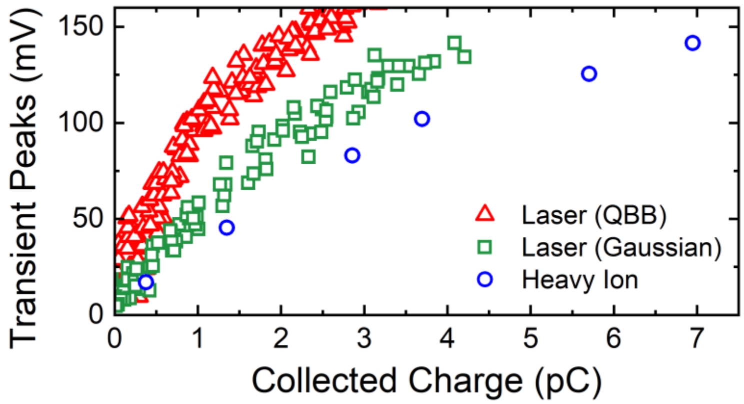

Fig. 31: Measured collector transient peaks as a function of collector collected charge for a Gaussian beam, a quasi-Bessel beam, and heavy ions.

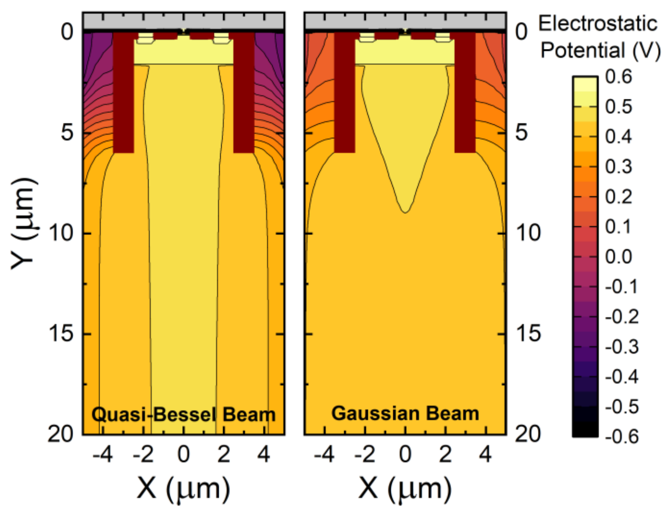

Fig. 32: Comparison of simulated electrostatic potential contours after 0.1 ns of peak charge deposition for a Quasi-Bessel beam (left) and a Gaussian beam (right). The contours shown are for charge deposition profiles that result in SETs of the same amplitude.

Summary

Throughout the duration of this program we have developed several simulation, experimental, and data analysis techniques that have been published and presented at several venues. The key achievements of this program can be listed as follows:

1. Developed advanced numerical and TCAD modeling techniques that were leveraged to understand the differences between charge collection resulting from charge deposited via ion and laser sources
2. Developed analytical expressions to calculated charge deposited in a semiconductor device by pulsed lasers
3. Developed a new data analysis approach that uses "feature matching" and allows for optimizing optical parameters to facilitate the correlation between ion and laser sources.

4. Developed a new experimental technique for charge deposition using an Axicon to better mimic the carrier densities generated by heavy ions
5. Established one-to-one correlations between laser pulse energy and heavy ion LET for several samples using both empirical and analytical methods
6. Advanced the understanding of fundamental charge collection mechanisms in several device types and semiconductor processes
7. Developed a new method to extract the spatial dependence of charge collection efficiency in a device using only pulsed laser measurements.
8. Tested and validated experimental techniques, data analysis approaches, and simulations across several platforms and types of devices

The work produced as a result of this program has contributed to expanding the body of work related to establishing a quantitative correlation between pulsed laser data and heavy-ion data. The understanding of several fundamental concepts needed for this effort were significantly advanced. In addition, many experimental challenges required to tackle these problems were addressed (e.g., improved calibration of a laser system). The successful outcome of this program was largely due to the synergistic collaboration between the teams at Georgia Tech and NRL.

The work completed and in progress has acquired a great deal of momentum and has garnered the interest of the radiation effects community. At this time, additional funding for these efforts would continue to build on this momentum and enable even more advancements in this area. The next steps in this work are to extend the methods and techniques developed in this program to the quantitative correlation of SEEs in circuits and systems, an area that would be of interest to the DoD.

What opportunities for training and professional development has the project provided?

The accomplishments and success of this program are a result of the work completed by a close collaboration between several students at Georgia Tech and research scientists at the U.S. Naval Research Laboratory. A list of training and professional development opportunities for the students are included below.

Mason Wachter

- Worked on project as an M.S. student
- Learned how to perform and completed pulsed-laser testing at NRL
- Oral presentation at RADECS 2016
- Completed his M.S. Degree

Zachary Fleetwood

- Worked on project as an M.S. and Ph.D. student

- Learned how to perform and completed heavy ion experiments at several facilities and pulsed-laser testing at NRL
- Several oral presentations at IEEE NSREC through the years
- Several publications in IEEE Transactions on Nuclear Science
- Completed his M.S. and Ph.D. degrees

Adrian Ildefonso

- Worked on project as an M.S. and Ph.D. student
- Learned how to perform and completed heavy ion experiments at several facilities and pulsed-laser testing at NRL
- Several oral presentations at IEEE NSREC through the years
- Several publications in IEEE Transactions on Nuclear Science
- Received direct mentoring from senior students and research scientists at NRL
- Completed two internships at NRL
- Completed his M.S. and Ph.D. degrees

George Tzintzarov

- Worked on project as a B.S., M.S., and Ph.D. student
- Learned how to perform and completed heavy ion experiments at several facilities and pulsed-laser testing at NRL
- Oral Presentation at IEEE NSREC 2019
- Several publications in IEEE Transactions on Nuclear Science
- Received direct mentoring from senior students and research scientists at NRL
- Completed his B.S. and M.S. degrees

Delgermaa Nergui

- Worked on project as a B.S. and M.S. student
- Learned how to perform and completed heavy ion experiments at several facilities and pulsed-laser testing at NRL
- Oral Presentation at IEEE NSREC 2019
- Several publications in IEEE Transactions on Nuclear Science
- Received direct mentoring from senior students and research scientists at NRL
- Completed her B.S. degree

How have the results been disseminated to communities of interest?

The results of this research have been disseminated to the radiation effects community via publications, presentations at the *IEEE Nuclear and Space Radiation Effects Conference (NSREC)*, the *IEEE Transactions on Nuclear Science*, and the Radiation Effects on Components and Systems (RADECS) Conference. A list of the publications resulting from this program is included below:

Journal Papers Published:

1. Z. E. Fleetwood, N. E. Lourenco, A. Ildefonso, J. H. Warner, M. T. Wachter, J. M. Hales, G. N. Tzintzarov, N. J. H. Roche, A. Khachatrian, S. P. Buchner, D. McMorrow, P. Paki, J. D. Cressler, "Using TCAD Modeling to Compare Heavy-Ion and Laser-Induced Single Event Transients in SiGe HBTs," in IEEE Transactions on Nuclear Science, vol.64, no.1, pp.398-405, Jan 2017.
2. J. M. Hales, A. Khachatrian, S. Buchner, N. J.-H. Roche, J. Warner, Z. E. Fleetwood, A. Ildefonso, J. D. Cressler, V. Ferlet-Cavrois, D. McMorrow, “Experimental Validation of an Equivalent LET Approach for Correlating Heavy-Ion and Laser-Induced Charge Deposition,” IEEE Transactions on Nuclear Science, vol. 65, no. 8, pp. 1724–1733, Aug. 2018.
3. A. Ildefonso, Z. E. Fleetwood, G. N. Tzintzarov, J. M. Hales, D. Nergui, M. Frounchi, A. Khachatrian, S. P. Buchner, D. McMorrow, J. H. Warner, J. Harms, A. Erickson, K. Voss, V. Ferlet-Cavrois, and J. D. Cressler, “Optimizing Optical Parameters to Facilitate Correlation of Laser- and Heavy-Ion-Induced Single-Event Transients in SiGe HBTs,” IEEE Trans. Nucl. Sci., vol. 66, no. 1, pp. 359–367, Jan. 2019.
4. J. M. Hales, A. Khachatrian, J. Warner, S. Buchner, A. Ildefonso, G. N. Tzintzarov, D. Nergui, D. M. Monahan, S. D. LaLumondiere, J. D. Cressler, D. McMorrow, “Using Bessel beams and two-photon absorption to predict radiation effects in microelectronics,” Opt. Express, vol. 27, no. 26, pp. 37 652–37 666, Dec. 2019.
5. J. M. Hales, A. Khachatrian, S. Buchner, J. H. Warner, A. Ildefonso, G. N. Tzintzarov, D. Nergui, D. M. Monahan, S. D. LaLumondiere, B. Lotshaw, J. D. Cressler, D. McMorrow, “New Approach for Pulsed-Laser Testing That Mimics Heavy-Ion Charge Deposition Proles,” IEEE Trans. Nucl. Sci., vol. 67, no. 1, pp. 81–90, Jan. 2020.
6. A. Ildefonso, G. N. Tzintzarov, A. P. Omprakash, D. Nergui, P. S. Goley, J. M. Hales, A. Khachatrian, S. P. Buchner, J. H. Warner, D. McMorrow, J. D. Cressler, “Comparison of Single-Event Transients in SiGe HBTs on Bulk and Thick-Film SOI,” IEEE Trans. Nucl. Sci., vol. 67, no. 1, pp. 71–80, Jan. 2020.
7. D. Nergui, A. Ildefonso, G. N. Tzintzarov, N. E. Lourenco, A. P. Omprakash, P. S. Goley, Z. E. Fleetwood, S. D. Lalumondiere, J. P. Bonsall, D. M. Monahan, H. Kettering, D. L. Brewe, J. D. Cressler, “Single-Event Transients in SiGe HBTs Induced by Pulsed X-Ray Microbeam,” IEEE Trans. Nucl. Sci., vol. 67, no. 1, pp. 91–98, Jan. 2020.
8. G. N. Tzintzarov, A. Ildefonso, P. S. Goley, M. Frounchi, D. Nergui, S. G. Rao, J. Teng, J. Campbell, A. Khachatrian, S. P. Buchner, D. McMorrow, J. H. Warner, M. Kaynak, L. Zimmermann, J. D. Cressler, “Electronic-to-Photonic Single-Event Transient Propagation Analysis in a Segmented Mach-Zehnder Modulator in a Si/SiGe Integrated Photonics Platform,” IEEE Trans. Nucl. Sci., vol. 67, no. 1, pp. 260–267, Jan. 2020.

9. A. Ildefonso, N. E. Lourenco, G. N. Tzintzarov, Z. E. Fleetwood, A. Khachatrian, S. P. Buchner, D. McMorrow, J. H. Warner, M. Kaynak, J. D. Cressler, "Tradeoffs Between RF Performance and SET Robustness in Low-Noise Amplifiers in a Complementary SiGe BiCMOS Platform," IEEE Trans. Nucl. Sci., vol. 67, no. 7, pp. 1521–1529, Jul. 2020.

Conference Papers Published:

1. Z. E. Fleetwood, N. E. Lourenco, **A. Ildefonso**, J. H. Warner, M. T. Wachter, J. M. Hales, G. N. Tzintzarov, N. J.-H. Roche, A. Khachatrian, S. P. Buchner, D. McMorrow, P. Paki, J. D. Cressler, "Using TCAD Modeling to Compare Heavy-Ion and Laser-Induced Single Event Transients in SiGe HBTs", Paper G-4, 2016 IEEE Nuclear and Space Radiation Effects Conference, 2016.
2. Z. E. Fleetwood, and J. D. Cressler, "Radiation Hardening and Heavy-ion to Laser Correlation in SiGe Devices and Circuits," Government Microcircuit Applications & Critical Technology Conference, 2017.
3. A. Ildefonso, Z. E. Fleetwood, G. N. Tzintzarov, J. M. Hales, D. Nergui, M. Frounchi, A. Khachatrian, S. P. Buchner, D. McMorrow, J. H. Warner, J. Harms, A. Erickson, K. Voss, V. Ferlet-Cavrois, J. D. Cressler, "Optimizing Optical Parameters to Facilitate Correlation of Laser- and Heavy-Ion-Induced Single-Event Transients in SiGe HBTs", Paper H-3, 2018 IEEE Nuclear and Space Radiation Effects Conference, Jul. 2018.
4. J. M. Hales, A. Khachatrian, S. Buchner, J. H. Warner, A. Ildefonso, G. N. Tzintzarov, D. Nergui, J. D. Cressler, D. McMorrow, "New Approach for Pulsed-Laser Testing That Mimics Heavy-Ion Charge Deposition Proles", Paper B-2, 2019 IEEE Nuclear and Space Radiation Effects Conference, Jul. 2019.
5. A. Ildefonso, G. N. Tzintzarov, A. P. Omprakash, D. Nergui, P. S. Goley, J. M. Hales, A. Khachatrian, S. P. Buchner, J. H. Warner, D. McMorrow, J. D. Cressler, "Comparison of Single-Event Transients in SiGe HBTs on Bulk and Thick-Film SOI", Paper B-1, 2019 IEEE Nuclear and Space Radiation Effects Conference, Jul. 2019.
6. D. Nergui, A. Ildefonso, G. N. Tzintzarov, A. P. Omprakash, Z. E. Fleetwood, S. D. Lalumondiere, J. P. Bonsall, D. M. Monahan, H. Kettering, D. L. Brewe, J. D. Cressler, "Single-Event Transients in SiGe HBTs Induced by Pulsed X-Ray Microbeam", Paper B-3, 2019 IEEE Nuclear and Space Radiation Effects Conference, Jul. 2019.
7. G. N. Tzintzarov, A. Ildefonso, P. S. Goley, M. Frounchi, J. Campbell, A. Khachatrian, S. P. Buchner, D. McMorrow, J. H. Warner, M. Kaynak, L. Zimmermann, J. D. Cressler, "Electronic-to-Photonic Single-Event Transient Propagation Analysis in a Segmented Mach-Zehnder Modulator in a Si/SiGe Integrated Photonics Platform", Paper H-1, 2019 IEEE Nuclear and Space Radiation Effects Conference, Jul. 2019.
8. A. Ildefonso, N. E. Lourenco, G. N. Tzintzarov, Z. E. Fleetwood, A. Khachatrian, S. P. Buchner, D. McMorrow, J. H. Warner, M. Kaynak, J. D. Cressler, "Tradeoffs Between RF Performance and SET Robustness in Low-Noise Amplifiers in a Complementary SiGe BiCMOS Platform", Paper D-4, Radiation Effects on Components and Systems (RADECS) Conference, Sep. 2019.

Conference Papers Accepted for Publication:

1. J. M. Hales, A. Khachatrian, J. Warner, S. Buchner, and D. McMorrow, "An improved approach for quantitative pulsed-laser single-event effects testing using two-photon absorption," in European Conference on Radiation and its Effects Components and Systems, Montpellier, France, In Press.
2. A. Ildefonso, G. N. Tzintzarov, D. Nergui, J. M. Hales, A. Khachatrian, A. Omprakash, S. P. Buchner, D. McMorrow, J. D. Cressler, "Laser-Induced Transients in SiGe HBTs Generated via Two-Photon Absorption Using Gaussian and Quasi-Bessel Beams", 2020 IEEE Nuclear and Space Radiation Effects Conference (NSREC), Accepted for Oral Presentation**.**
3. G. N. Tzintzarov, A. Ildefonso, J. W. Teng, M. Frounchi, A. Djikeng, P. Iyengar, P. S. Goley, R. Bahr, A. Khachatrian, S. P. Buchner, D. McMorrow, J. D. Cressler, "Optical Single-Event Transients Induced in Silicon-Photonic Waveguides by Two-Photon Absorption", 2020 IEEE Nuclear and Space Radiation Effects Conference (NSREC), Accepted for Oral Presentation.
4. D. Nergui, A. Ildefonso, G. N. Tzintzarov, A. Omprakash, J. D. Cressler, "An Investigation of SET Charge Transport Mechanisms in SiGe HBTs", 2020 IEEE Nuclear and Space Radiation Effects Conference (NSREC), Accepted for Poster Presentation.
5. J. M. Hales, A. Khachatrian, S. Buchner, D. M. Monahan, S. D. LaLumondiere, and D. McMorrow, "Mapping the Spatial Dependence of Charge Collection Efficiency in Devices Using Pulsed-Laser Testing", 2020 IEEE Nuclear and Space Radiation Effects Conference (NSREC), Accepted for Oral Presentation.

Awards Received

1. Zachary Fleetwood received the IEEE NPSS Graduate Scholarship Award in 2016.
2. Zachary Fleetwood received the IEEE NPSS Paul Phelps Continuing Education Grant in 2016.
3. George Tzintzarov received the NSF Graduate Research Fellowship in 2017.
4. Delgermaa Nergui received a travel award to the International Microwave Symposium through Project Connect in 2018.
5. Adrian Ildefonso received the IEEE NPSS Graduate Scholarship Award in 2018.
6. Adrian Ildefonso received the IEEE NPSS Paul Phelps Continuing Education Grant in 2018.
7. 2018 NSREC Outstanding Student Paper Award and Outstanding Conference Paper Award: A. Ildefonso, Z. E. Fleetwood, G. N. Tzintzarov, J. M. Hales, D. Nergui, M. Frounchi, A. Khachatrian, S. P. Buchner, D. McMorrow, J. H. Warner, J. Harms, A. Erickson, K. Voss, V. Ferlet-Cavrois, and J. D. Cressler for their paper entitled "Optimizing Optical Parameters to Facilitate Correlation of Laser- and Heavy-Ion-Induced Single-Event Transients in SiGe HBTs."
8. 2019 NSREC Outstanding Conference Paper Award: Joel M. Hales, Ani Khachatrian, Stephen Buchner, Jeffrey Warner, Adrian Ildefonso, George N. Tzintzarov, Delgermaa Nergui, Daniele M. Monahan, Stephen D. LaLumondiere, John D. Cressler, and Dale McMorrow for their paper entitled "New approach for pulsed-laser testing that mimics heavy-ion charge deposition profiles."
9. George Tzintzarov received the IEEE NPSS Paul Phelps Continuing Education Grant in 2019.